



## The effect of near-infrared fluorescence conjugation on the anti-cancer potential of cetuximab

Ji Young Yun<sup>1,2</sup>, Byung-Hwa Hyun<sup>2</sup>, Sang Yoon Nam<sup>1</sup>, Young Won Yun<sup>1</sup>,  
Hu-Jang Lee<sup>3,\*</sup>, Beom-Jun Lee<sup>1,\*</sup>

<sup>1</sup>College of Veterinary Medicine and Research Institute of Veterinary Medicine, Chungbuk National University, Cheongju, Korea

<sup>2</sup>Laboratory Animal Center, Osong Medical Innovation Foundation, Cheongju, Korea

<sup>3</sup>College of Veterinary Medicine and Institute of Animal Medicine, Gyeongsang National University, Jinju, Korea

This study investigated the anti-cancer potential of a near-infrared fluorescence (NIRF) molecule conjugated with Cetuximab (Cetuximab-NIRF) in six-week-old female BALB/c athymic (nu+/nu+) nude mice. A431 cells were cultured and injected into the animals to induce solid tumors. Paclitaxel (30 mg/kg body weight (BW)), Cetuximab (1 mg/kg BW), and Cetuximab-NIRF (0.25, 0.5 and 1.0 mg/kg BW) were intraperitoneally injected twice a week into the A431 cell xenografts of the nude mice. Changes in BW, tumor volume and weight, fat and lean mass, and diameter of the peri-tumoral blood vessel were determined after two weeks. Tumor volumes and weights were significantly decreased in the Cetuximab-NIRF (1 mg/kg BW) group compared with the control group ( $P < 0.001$ ). Lean mass and total body water content were also conspicuously reduced in the Cetuximab-NIRF (1 mg/kg BW) group compared with the vehicle control group. Peri-tumoral blood vessel diameters were very thin in the Cetuximab-NIRF groups compared with those of the paclitaxel group. These results indicate that the conjugation of Cetuximab with NIRF does not affect the anti-cancer potential of Cetuximab and NIRF can be used for molecular imaging in cancer treatments.

**Keywords:** Anti-cancer, near-infrared fluorescence, Cetuximab-NIRF, A431 cells

Received 30 January 2018; Revised version received 27 February 2018; Accepted 28 February 2018

The epidermal growth factor receptor (EGFR) plays a crucial role in the development and progression of human carcinomas, and its overexpression is usually associated with poor prognosis [1]. Cetuximab (Erbix<sup>®</sup>) is a chimeric anti-EGFR monoclonal antibody used in the treatment of metastatic colorectal cancer and head and neck cancer [1,2]. Anti-EGFR antibody treatment causes an increase in the expression of the cell-cycle inhibitor p27kip1 [3]. Cetuximab treatment has similar antiproliferative effects by increasing p27kip1 levels and reducing proliferating cell nuclear antigen expression in human tumor xenografts in nude mice [4]. In addition, Cetuximab resulted in a significant decrease in the

production of angiogenic factors in an A431 tumor xenograft model [5,6].

Cell survival is dependent, in part, upon the ratio of Bax, which promotes apoptosis, to Bcl-2, which protects cells from apoptosis [7]. Several reports have shown that treatment with Cetuximab or similar anti-EGFR antibodies may alter the balance of Bax and Bcl-2 expression [8]. Cetuximab has been shown to increase the incidence of human tumor-cell apoptosis both *in vitro* and *in vivo* in a number of model systems [9].

The expression level of EGFR is not correlated with the clinical response to Cetuximab [10]. Thus, EGFR expression is not a predictor of tumor response [11].

\*Corresponding authors: Beom-Jun Lee, College of Veterinary Medicine, Chungbuk National University, 1 Chungdae-ro, Seowon-gu, Cheongju 28644, Korea

Tel: +82-43-261-3357; Fax: +82-43-271-3246; E-mail: beomjun@cbu.ac.kr

Hu-Jang Lee, College of Veterinary Medicine, Gyeongsang National University, 501 Jinjudae-ro, Jinju 52828, Korea

Tel: +82-55-772-2352; Fax: +82-55-772-2308; E-mail: hujang@gnu.ac.kr

This is an Open Access article distributed under the terms of the Creative Commons Attribution Non-Commercial License (<http://creativecommons.org/licenses/by-nc/3.0>) which permits unrestricted non-commercial use, distribution, and reproduction in any medium, provided the original work is properly cited.

These observations, together with the side effects and high costs of mAb-based immunotherapy, have necessitated investigations into the early predictive biomarkers of tumor response to Cetuximab therapy [12].

Investigation of the many fundamental processes in life sciences requires straightforward tools for fast, sensitive, reliable, and reproducible detection of biomolecular interaction among various molecular or ionic species. One of the best suited and most popular methods to meet these challenges is the use of photoluminescence or fluorescence techniques in conjunction with functional dyes and labels [13,14]. Fluorescence detection is by far the most dominant detection method in the field of sensing technology due to several well-established advantages. However, it can be difficult to achieve a low detection limit in fluorescence detection due to the limited extinction coefficients or quantum yields of traditional organic dyes, as well as a low dye-to-reporter molecule labeling ratio. The recent explosion of nanotechnology, leading to the development of materials with submicrometer-sized dimensions and unique optical properties, has opened up new horizons for fluorescence detection [15].

Molecular imaging can non-invasively detect molecular changes during cancer treatment, which occur earlier than anatomical changes, such as decrease in tumor volume [16]. Compared with positron emission tomography and single-photon-emission computed tomography, optical imaging techniques, such as near-infrared fluorescence (NIRF) imaging, are limited in the depth of tissue penetration and are not routine clinical modalities. However, NIRF does not require the use of radioactive materials. Optical imaging also facilitates multicolor imaging using fluorophores with different emission wavelengths [17].

In this study, we investigated the anti-cancer effect of Cetuximab conjugated with NIRF on A431 tumor xenografts in nude mice. Changes in tumor volume and weight, and as well as the diameter of peri-tumoral blood vessel were determined using a nuclear magnetic resonance (NMR)-based body composition analyzer and confocal endomicroscopy.

## Materials and Methods

### Anti-cancer reagents

Paclitaxel (solid; batch 80617492D, purity >98%), commercially available paclitaxel formulated in Kolliphor EL-dehydrated ethanol USP (1:1 (v/v), Taxol), and 2'-

methylpaclitaxel were obtained from Sigma-Aldrich Co. Ltd. (Darmstadt, Germany). The other chemicals were of analytical gradient grade, and originated from Sigma Chemical Co. (St. Louis, MO, USA). Purified deionized water was prepared using the Milli-Q Plus system (Waters, Milford, MA, USA).

Clinical-grade Cetuximab was supplied by ImClone Systems (New York, NY, USA) at a concentration of 2 mg/mL in a phosphate buffer solution (PBS, pH 7.2). For tests requiring lower concentrations of Cetuximab, the stock solution was diluted with sterile PBS (pH 7.4). Cetuximab was administered intraperitoneally at a constant volume of 0.5 mL per mouse.

### Mice

Sixty specific pathogen-free (SPF) female BALB/c athymic (nu+/nu+) mice (5–6 weeks old, 18–20 g) were purchased from Nara Biotech (Seoul, Korea). Mice were allowed to acclimatize to local conditions for 1 week. Mice were housed in air-filtered laminar flow cabinets and handled using aseptic procedures with a 12/12-h light/dark cycle at 21±2°C and food and water *ad libitum*. All animal experiments complied with the requirements of the Animal Care and Ethics Committees of Chungbuk National University.

### Cell culture

A431 cells were purchased from the American Type Culture Collection (Manassas, VA, USA). Cells were incubated in a 5% CO<sub>2</sub>/95% air atmosphere at 37°C in a one-to-one mixture of Ham's F12 and Dulbecco-Modified Eagle's Medium (DMEM) (Sigma-Aldrich, Darmstadt, Germany) supplemented with 1.2 g of sodium bicarbonate per liter, 15 mM HEPES, and penicillin. To initiate the experiments, cells were detached from stock flasks using a solution of 0.1% crude trypsin and 0.9 mM EDTA in PBS, suspended in an equal volume of medium containing 0.1% soybean trypsin inhibitor, centrifuged out of suspension, and transferred to a T75-T225 cell culture flask in suitable media. Where indicated, bovine insulin, human transferrin, human CIg, and ethanolamine were added directly to culture plates containing 1 mL of the medium as small volumes of sterile, 100-fold concentrated stocks shortly before adding cells to a second milliliter of the medium. Final concentrations were 10 pg/mL insulin, 10 pg/mL transferrin, 5 pg/mL CIg, and 0.5 mM ethanolamine. Epidermal growth factor (EGF) was added as small volumes of

sterile, concentrated stocks to give the indicated final concentrations. Fetal bovine serum (FBS) was added to give a final concentration of 10%. To determine the cell number at the logarithmic growth phase, cells were detached from plates using the trypsin-EDTA-PBS solution, and suspensions were counted in a hemocytometer (Sigma-Aldrich, Darmstadt, Germany).

### Xenograft of A431 cells in nude mice

After acclimation for 1 week, mice were anesthetized using 2% isoflurane with oxygen for tail vein injection. To generate the mouse cancer models, A431 cells ( $3 \times 10^7$ ) were subcutaneously implanted into the right flank. After tumors were allowed to reach a predetermined size (100 to 200 mg), the animals were divided into six groups ( $n=10$  per group): saline (CON), paclitaxel (30 mg/kg BW, PAC), Cetuximab (1 mg/kg BW, CET), and Cetuximab-NIRF (0.25 (CN-0.25), 0.5 (CN-0.5), and 1 (CN-1.0) mg/kg BW) were treated by intraperitoneal injection once a day for 13 days. Treatment of each animal was based on the individual BW basis for each drug.

### Measurement of tumor size, body fat and lean mass

Treated animals were checked daily for treatment-related toxicity and mortality. In addition, the average BW for each group was determined before initiation of treatment (Wt1) and following the last treatment dose (Wt2). The difference in BW (Wt2-Wt1) was then used to estimate the degree of treatment-related toxicity. Tumor size was measured with a caliper twice a week, until they reached a predetermined “target” size (0.5-1 g depending on the tumor model used). tumor volume ( $\text{mm}^3$ ) was calculated using the following formula:  $(L \times H \times W)/2$ , where L is the length, W the width, and H the height of the tumor in millimeters.

All mice were sacrificed at the end of treatment, and their tumors were harvested for analysis. Changes in fat and lean mass and total body water of mice were also determined using the NMR-based body composition analyzer (Echo Medical Systems, Houston, TX, USA).

### Confocal microscopy

During the intervention period, growth of endometriotic lesions was monitored by measuring the bioluminescence of the subcutaneous luciferase-positive implants using a non-invasive IVIS 200 live animal imaging system (Xenogen Corp., Alameda, CA, USA). A total of 100

mg/kg of luciferin was intravenously injected into the mouse tail vein 10 min prior to imaging. An image from each animal was captured at bin size 4 in triplicate, and the bioluminescence signal intensities were averaged for comparison. At the end of the intervention, functional angiogenesis of endometriotic lesions was monitored by measuring the flow of fluorescence dye in the new microvessels formed in the implants using a Cellvizio LAB LSU-488 system with a ProFlex Microprobe S1500 (Mauna Kea Technologies, Paris, France).

### Statistical analysis

All data were presented as mean  $\pm$  standard deviation (SD). Statistical analyses were carried out using one-way analysis of variance (ANOVA) with the computer software SPSS 12.0 (SPSS Inc., Chicago, IL, USA) and Student's t-test to compare significances among different groups. For all tests, results were considered statistically significant when  $P < 0.05$ .

## Results

### BW changes

As shown in Figure 1, changes in the mean BW of all groups were determined by BW 2, 6, 9 and 13 days after administration of the drug. On the 2nd day post-treatment, the BW in PAC was significantly decreased compared with that in CON. At 6 days post-treatment, the BW in CN-0.5 was significantly increased compared with that in CON. In addition, the BW in CN-0.25 and CN-0.5 was significantly increased compared with that

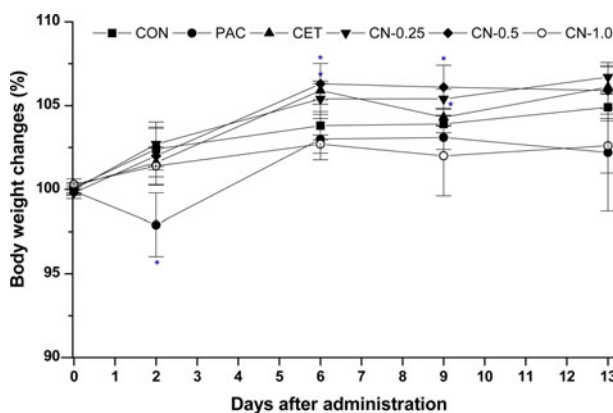


**Figure 1.** Body weight changes from treatment with saline (CON), paclitaxel (30 mg/kg) (PAC), cetuximab (1 mg/kg) (CET), and cetuximab-NIRF (0.25 (CN-0.25), 0.5 (CN-0.5), and 1.0 (CN-1.0) mg/kg) for 14 days in nude mice. \* $P < 0.05$  and \*\* $P < 0.01$  vs. CON at the corresponding time points.

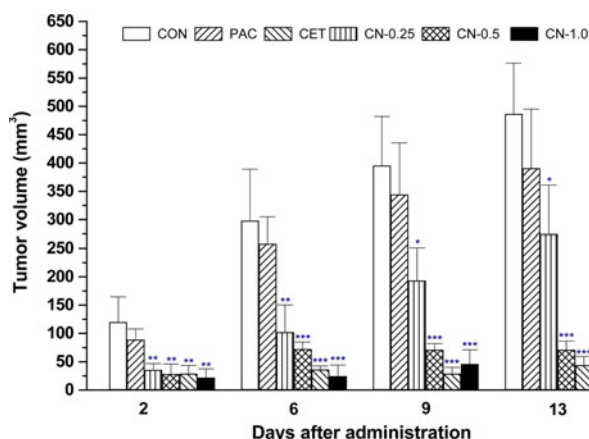


**Figure 2.** Tumor volume changes from treatment with saline (CON), paclitaxel (30 mg/kg) (PAC), cetuximab (1 mg/kg) (CET), and cetuximab-NIRF (0.25 (CN-0.25), 0.5 (CN-0.5), and 1.0 (CN-1.0) mg/kg) for 13 days on A431 xenografts in nude mice. \* $P < 0.05$ , \*\* $P < 0.01$  and \*\*\* $P < 0.001$  vs. CON at the corresponding time points.

in CON at 9 days post-administration. However, there was no significant difference between CON and all treated groups at 13 days post-treatment.

### Tumor volume changes

The therapeutic efficacy of paclitaxel, Cetuximab and Cetuximab-NIRF was investigated in mice bearing A431 xenografts. Figure 2 shows changes in tumor volume on A431 xenografts in nude mice treated with several drugs. At 2 days post-treatment, the tumor volume of CET, CN-0.25, CN-0.5 and CN-1.0 was significantly decreased compared with that of CON ( $P < 0.01$ ). At 6 days post-administration, the tumor volume of CET ( $P < 0.001$ ), CN-0.25 ( $P < 0.01$ ), CN-0.5 ( $P < 0.001$ ) and CN-1.0 ( $P < 0.001$ ) was significantly decreased compared with that of CON. In addition, the tumor volume of CET ( $P < 0.001$ ), CN-0.25 ( $P < 0.05$ ), CN-0.5 ( $P < 0.001$ ) and CN-1.0 ( $P < 0.001$ ) was significantly decreased compared with that of CON at 9 and 13 days post-treatment. At the end of drug treatment, there was no significant difference in tumor volume between CET and CN-1.0.

### Tumor weight

Tumor weight was further confirmed at the end of the experiment after sacrificing the mice. Figure 3 shows the weight of the tumor mass on A431 xenografts in nude mice treated with several drugs at the end of the experiment. The tumor mass weight of CET ( $P < 0.001$ ), CN-0.25 ( $P < 0.05$ ), CN-0.5 ( $P < 0.001$ ) and CN-1.0

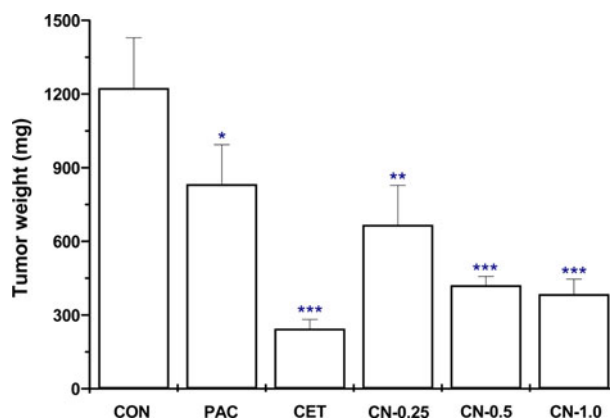


**Figure 3.** Tumor weight changes from treatment with saline (CON), paclitaxel (30 mg/kg) (PAC), cetuximab (1 mg/kg) (CET), and cetuximab-NIRF (0.25 (CN-0.25), 0.5 (CN-0.5), and 1.0 (CN-1.0) mg/kg) for 13 days on A431 xenografts in nude mice. \* $P < 0.05$ , \*\* $P < 0.01$  and \*\*\* $P < 0.001$  vs. CON at the corresponding time points.

( $P < 0.001$ ) was significantly decreased compared with that of CON. However, there was no significant difference in the tumor mass weight between CON and PAC.

### Effect on angiogenesis

Figure 4 shows the change in tumor blood vessel diameters (A) and an image of tumor angiogenesis by confocal endomicroscopy (B) on A431 xenografts in nude mice treated with several drugs. The tumor blood vessel diameter of CET ( $P < 0.05$ ), CN-0.5 ( $P < 0.001$ ) and CN-1.0 ( $P < 0.001$ ) was significantly decreased compared with that of CON. However, the tumor blood vessel diameter of PAC was increased, but there was no significant difference between PAC and CON. As shown in Figure 4B, treatment with CET, CN-0.5 and CN-1.0 resulted in a tremendous decrement in the number of blood vessels around the tumor mass.

## Discussion

Cetuximab is a chimeric mouse/human monoclonal antibody of the immunoglobulin G1 (IgG1) subclass that targets the human epidermal growth factor receptor (EGFR) [18]. The present study investigated the anti-tumoral effect of Cetuximab conjugated to a molecular imaging material for targeted treatment of tumor cells compared with the original biological-activities of Cetuximab. In this study, the results indicate that NIRF can be used as a promising theranostic nanomedicine for curative targeting of EGFR-expressing tumor cells in

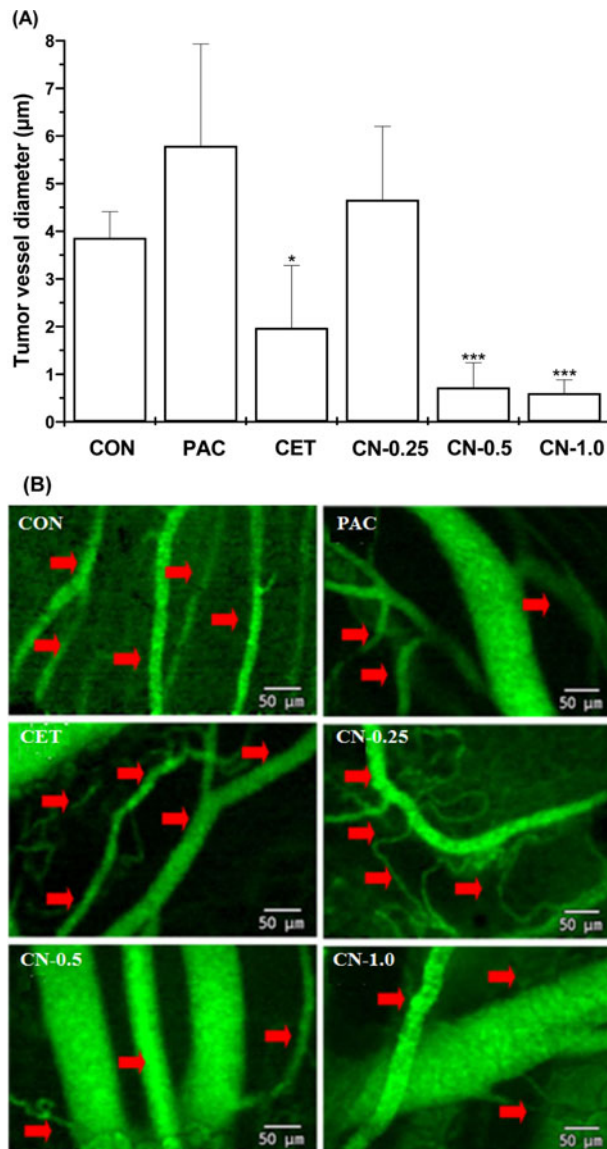


**Figure 4.** Changes in tumor blood vessel diameter (A) and image of tumor angiogenesis by confocal endomicroscopy on A431 xenografts in nude mice treated with saline (CON), paclitaxel (30 mg/kg) (PAC), cetuximab (1 mg/kg) (CET), and cetuximab-NIRF (0.25 (CN-0.25), 0.5 (CN-0.5) and 1.0 (CN-1.0) mg/kg) for 13 days. \* $P < 0.05$ , \*\* $P < 0.01$  and \*\*\* $P < 0.001$  vs. CON at the corresponding time points.

*in vivo* using the therapeutic antibody Cetuximab and non-invasive monitoring of treatment efficacy. Several clinical studies have shown that Cetuximab is capable of significantly inhibiting tumor growth [19,20]. In addition, most patients who receive Cetuximab manifest either intrinsic resistance or acquired resistance after initially demonstrating positive results [19-21]. Therefore, EGFR expression is not a predictor of tumor response. These observations, together with the side effects and high

costs of immunotherapy, have necessitated investigations into the early predictive biomarkers of tumor response to Cetuximab therapy.

Accordingly, the results from this study could provide important findings relevant to the potential conjugating/functioning effects of the chimeric EGFR antibody Cetuximab. The *in vivo* assays performed to assess the effect of Cetuximab and conjugated-Cetuximab had apparent similarities. In a previous study [20], a method was developed to image tumor-associated lysosomal protease activity as a xenograft mouse model *in vivo* using autoquenched NIRF probes. Furthermore, NIRF probes were bound to a long circulating graft copolymer consisting of poly-L-lysine and methoxypolyethylene glycol succinate [22]. Following intravenous injection, the NIRF probe carrier accumulated in solid tumors due to its long circulation time and leakage through tumor neovasculature. An intratumoral NIRF signal was generated by lysosomal proteases in tumor cells [20].

In this study, enhancement of the anti-proliferative effects was observed by using combined agents (Cetuximab-NIRF (CET-NIRF)) compared with either paclitaxel or Cetuximab alone, as measured by confocal microscopy. In addition, combined modality therapy had a significant impact on the growth of A431 tumor cells in an *in vivo* xenograft model. There was a significant decrease in tumor volume and size when the antibody was conjugated with NIRF material. CET-NIRF at a concentration of 1.0 mg/kg BW provided the same effective anticancer potential demonstrated by tumor volume and weight changes. A number of investigators have shown interactions between Cetuximab and various chemotherapeutic agents. However, most of these studies were initiated at a much earlier stage and in the presence of non-palpable tumors or small tumor burden [23,24].

In mice models, the results from this study suggest that CET-NIRF can conspicuously inhibit tumor growth. The main mechanism is probably associated with the larger intracellular volume of Cetuximab, which benefits from the internalized NIRF materials. It was also proven that NIRF materials can bind to vascular endothelial growth factor (VEGF) and inhibit cell angiogenic activity, which is a key step involved in tumor formation [25,26].

A previous study [27] demonstrated that angiogenesis is vital process during tumor development. The currently accepted standard method for quantifying tumor angiogenesis is to assess microvessel density (MVD) based on CD105 staining, which is an independent

prognostic factor for survival in patients with most solid tumor types. This is the first successful NIRF imaging study of CD105 expression *in vivo* [28]. Fast, prominent, persistent, and CD105-specific uptake of the probe during tumor angiogenesis was observed in a mouse model [29]. To confirm the original biological-activities of cetuximab and the EGFR-targeted probe for optical imaging of CET-NIRF, the present study assessed the perivascular angiogenesis of the tumor from changes in blood vessel diameter measured by confocal endomicroscopy. The rationale for choosing the A431 tumor model for this study is that the parent antibody of Cetuximab has been shown to be an effective anti-angiogenic agent in this model. Perivascular diameter in CET was significantly decreased compared with that in CON ( $P < 0.05$ ). Furthermore, treatment with CN-0.5 and CN-1.0 resulted in a tremendous decrement in the size and/or number of blood vessels around the tumor mass. Based on these results, CET-NIRFs significantly inhibit cell proliferation, weaken migration and simultaneously accelerate Cetuximab-induced apoptosis without affecting cell cycle arrest, as seen by the tumor volume and weight change findings.

The antitumor activity of Cetuximab, including G0/G1 cell-cycle arrest, induction of apoptosis, inhibition of DNA repair, inhibition of angiogenesis, and inhibition of tumor cell motility, invasion, and metastasis, has been demonstrated in preclinical models [30]. In Cetuximab-modified NIRFs, Cetuximab can function as a targeting moiety for recognizing EGFR-overexpressing cells, and bring about other therapeutic and diagnostic effects [31]. These effects have been reported in Cetuximab-conjugated NIRF molecules, which are able to target EGFR *in vivo*, leading to an increase in the target/non-target distribution ratio, enhancing cellular internalization of the targeted nanoparticles, and improving imaging signals [31,32].

Based on our overall results, it is evident that NIRF molecules can be an excellent candidate for use in EGFR-targeted probe for optical imaging, as the functionalization (conjugation) of newly synthesized NIRF molecule does not affect the original biological-activities of Cetuximab.

## Acknowledgments

This work was supported by a research grant from Chungbuk National University in 2014.

**Conflict of interests** The authors declare that there is no financial conflict of interests to publish these results.

## References

1. Arteaga CL. EGF receptor as a therapeutic target: patient selection and mechanisms of resistance to receptor-targeted drugs. *J Clin Oncol* 2003; 21(23 Suppl): 289s-291s.
2. Wheeler DL, Dunn EF, Harari PM. Understanding resistance to EGFR inhibitors-impact on future treatment strategies. *Nat Rev Clin Oncol* 2010; 7(9): 493-507.
3. Peng D, Fan Z, Lu Y, DeBlasio T, Scher H, Mendelsohn J. Anti-epidermal growth factor receptor monoclonal antibody 225 up-regulates p27KIP1 and induces G1 arrest in prostatic cancer cell line DU145. *Cancer Res* 1996; 56(16): 3666-3669.
4. Fagin JA. The Jeremiah Metzger lecture: intelligent design of cancer therapy: trials and tribulations. *Trans Am Clin Climatol Assoc* 2007; 118: 253-261.
5. Perrotte P, Matsumoto T, Inoue K, Kuniyasu H, Eve BY, Hicklin DJ, Radinsky R, Dinney CPN. Anti-epidermal growth factor receptor antibody C225 inhibits angiogenesis in human transitional cell carcinoma growing orthotopically in nude mice. *Clin Cancer Res* 1999; 5(2): 257-265.
6. Petit AM, Rak J, Hung MC, Rockwell P, Goldstein N, Fendly B, Kerbel RS. Neutralizing antibodies against epidermal growth factor and ErbB-2/neu receptor tyrosine kinases down-regulate vascular endothelial growth factor production by tumor cells *in vitro* and *in vivo*: angiogenic implications for signal transduction therapy of solid tumors. *Am J Pathol* 1997; 151(6): 1523-1530.
7. Pepper C, Hoy T, Bentley DP. Bcl-2/Bax ratios in chronic lymphocytic leukaemia and their correlation with *in vitro* apoptosis and clinical resistance. *Br J Cancer* 1997; 76(7): 935-938.
8. Wu X, Fan Z, Masui H, Rosen N, Mendelsohn J. Apoptosis induced by an anti-epidermal growth factor receptor monoclonal antibody in a human colorectal carcinoma cell line and its delay by insulin. *J Clin Invest* 1995; 95(4): 1897-1905.
9. Ciardiello F, Bianco R, Damiano V, De Lorenzo S, Pepe S, De Placido S, Fan Z, Mendelsohn J, Bianco AR, Tortora G. Antitumor activity of sequential treatment with topotecan and anti-epidermal growth factor receptor monoclonal antibody C225. *Clin Cancer Res* 1999; 5(4): 909-916.
10. Wild R, Fager K, Flefleh C, Kan D, Inigo I, Castaneda S, Luo FR, Camuso A, McGlinchey K, Rose WC. Cetuximab preclinical antitumor activity (monotherapy and combination based) is not predicted by relative total or activated epidermal growth factor receptor tumor expression levels. *Mol Cancer Ther* 2006; 5(1): 104-113.
11. Saltz LB, Meropol NJ, Loehrer PJ Sr, Needle MN, Kopit J, Mayer RJ. Phase II trial of cetuximab in patients with refractory colorectal cancer that expresses the epidermal growth factor receptor. *J Clin Oncol* 2004; 22(7): 1201-1208.
12. Cunningham D, Humblet Y, Siena S, Khayat D, Bleiberg H, Santoro A, Bets D, Mueser M, Harstrick A, Verslype C, Chau I, Van Cutsem E. Cetuximab monotherapy and cetuximab plus irinotecan in irinotecan-refractory metastatic colorectal cancer. *N Engl J Med* 2004; 351(4): 337-345.
13. Resch-Genger U, Grabolle M, Cavaliere-Jaricot S, Nitschke R, Nann T. Quantum dots versus organic dyes as fluorescent labels. *Nat Methods* 2008; 5(9): 763-775.
14. Zhang J, Campbell RE, Ting AY, Tsien RY. Creating new fluorescent probes for cell biology. *Nat Rev Mol Cell Biol* 2002; 3(12): 906-918.
15. Waggoner A. Fluorescent labels for proteomics and genomics. *Curr Opin Chem Biol* 2006; 10(1): 62-66.

16. Cai W, Chen X. Multimodality molecular imaging of tumor angiogenesis. *J Nucl Med* 2008; 49(2 Suppl): 113S-128S.
17. Barrett T, Koyama Y, Hama Y, Ravizzini G, Shin IS, Jang BS, Paik CH, Urano Y, Choyke PL, Kobayashi H. *In vivo* diagnosis of epidermal growth factor receptor expression using molecular imaging with a cocktail of optically labeled monoclonal antibodies. *Clin Cancer Res* 2007; 13(22 Pt 1): 6639-6648.
18. Mendelsohn J. The epidermal growth factor receptor as a target for cancer therapy. *Endocr Relat Cancer* 2001; 8(1): 3-9.
19. Ma T, Liu H, Sun X, Gao L, Shi J, Zhao H, Jia B, Wang F, Liu Z. Serial *in vivo* imaging using a fluorescence probe allows identification of tumor early response to cetuximab immunotherapy. *Mol Pharm* 2015; 12(1): 10-17.
20. Weissleder R, Tung CH, Mahmood U, Bogdanov A Jr. *In vivo* imaging of tumors with protease-activated near-infrared fluorescent probes. *Nat Biotechnol* 1999; 17(4): 375-378.
21. Van Emburgh BO, Sartore-Bianchi A, Di Nicolantonio F, Siena S, Bardelli A. Acquired resistance to EGFR-targeted therapies in colorectal cancer. *Mol Oncol* 2014; 8(6): 1084-1094.
22. Wunder A, Tung CH, Müller-Ladner U, Weissleder R, Mahmood U. *In vivo* imaging of protease activity in arthritis: a novel approach for monitoring treatment response. *Arthritis Rheum* 2004; 50(8): 2459-2465.
23. Baselga J, Norton L, Masui H, Pandiella A, Coplan K, Miller WH Jr, Mendelsohn J. Antitumor effects of doxorubicin in combination with anti-epidermal growth factor receptor monoclonal antibodies. *J Natl Cancer Inst* 1993; 85(16): 1327-1333.
24. Fan Z, Baselga J, Masui H, Mendelsohn J. Antitumor effect of anti-epidermal growth factor receptor monoclonal antibodies plus cis-diamminedichloroplatinum on well established A431 cell xenografts. *Cancer Res* 1993; 53(19): 4637-4642.
25. Mukherjee P, Bhattacharya R, Wang P, Wang L, Basu S, Nagy JA, Atala A, Mukhopadhyay D, Soker S. Antiangiogenic properties of gold nanoparticles. *Clin Cancer Res* 2005; 11(9): 3530-3534.
26. Takata M, Chikumi H, Miyake N, Adachi K, Kanamori Y, Yamasaki A, Igishi T, Burioka N, Nanba E, Shimizu E. Lack of AKT activation in lung cancer cells with EGFR mutation is a novel marker of cetuximab sensitivity. *Cancer Biol Ther* 2012; 13(6): 369-378.
27. Folkman J. Angiogenesis in cancer, vascular, rheumatoid and other disease. *Nat Med* 1995; 1(1): 27-31.
28. Fonsatti E, Nicolay HJ, Altomonte M, Covre A, Maio M. Targeting cancer vasculature via endoglin/CD105: a novel antibody-based diagnostic and therapeutic strategy in solid tumours. *Cardiovasc Res* 2010; 86(1): 12-19.
29. Yang Y, Zhang Y, Hong H, Liu G, Leigh BR, Cai W. *In vivo* near-infrared fluorescence imaging of CD105 expression during tumor angiogenesis. *Eur J Nucl Med Mol Imaging* 2011; 38(11): 2066-2076.
30. Bandyopadhyay D, Mandal M, Adam L, Mendelsohn J, Kumar R. Physical interaction between epidermal growth factor receptor and DNA-dependent protein kinase in mammalian cells. *J Biol Chem* 1998; 273(3): 1568-1573.
31. Tseng SH, Chou MY, Chu IM. Cetuximab-conjugated iron oxide nanoparticles for cancer imaging and therapy. *Int J Nanomedicine* 2015; 10: 3663-3685.
32. Conde J, Bao C, Cui D, Baptista PV, Tian F. Antibody-drug gold nanoantennas with Raman spectroscopic fingerprints for *in vivo* tumour theranostics. *J Control Release* 2014; 183: 87-93.